Structural Engineering and Mechanics, Vol. 27, No. 6 (2007) 651-670
DOI: http://dx.doi.org/10.12989/sem.2007.27.6.651

After-fracture redundancy in simple span two-girder steel bridge

Yong-Myung Park† and Woom-Do-Ji Joe‡

Department of Civil Engineering, Pusan National University, 30 Jangjeon-dong, Geumjeong-gu, Busan 609-735, Korea

Min-Oh Hwang‡† and Tae-Yang Yoon‡‡

Civil Engineering Research Team, Research Institute of Industrial Science and Technology, 79-5 Youngcheon, Dongtan, Hwaseong, Gyeonggi-do 445-813, Korea

(Received September 18, 2006, Accepted June 29, 2007)

Abstract. An experimental study to evaluate a redundancy capacity in simple span two plate-girder bridges, which are generally classified as a non-redundant load path structure, has been performed under the condition that one of the two girders is seriously damaged. The bottom lateral bracing was selected as an experimental parameter and two 1/5-scale bridge specimens with and without bottom lateral bracing have been prepared. The loading tests were first performed on the intact specimens without cracked girder within elastic range. Thereafter, the ultimate loading tests were conducted on the damaged specimens with an induced crack at the center of a girder. The test results showed that the cross beams and concrete deck redistributed partly the applied load to the uncracked girder, but the lateral bracing system played a significant role of the load redistribution when a girder was damaged. The redundancy was evaluated based on the test results and an appropriate redundancy level was evaluated when the lateral bracing was provided in a seriously damaged simple span two-girder steel bridge.

Keywords: redundancy; simple span two-girder bridge; bottom lateral bracing; fractured girder; load redistribution.

1. Introduction

AASHTO standard specifications (2002) and LRFD specifications (2004) for highway bridges classify all two-girder steel highway bridges as non-redundant whether they are simple span or continuous. However, experiences show that two-girder bridges typically do not collapse following fracture of a girder. In fact, not only do they remain serviceable in some cases, but damage sometimes is not even suspected until the fracture is discovered incidentally or during an inspection (Daniels *et al.* 1989, McGormley *et al.* 2000). This is due to, so called, the redundancy of bridge system.

† Associate Professor, E-mail: ympk@pusan.ac.kr
‡ Ph.D. Student, E-mail: woomdoji@pusan.ac.kr
‡† Senior Researcher, E-mail: mohwang@rist.re.kr
‡‡ Director, Corresponding author, E-mail: tyoon@rist.re.kr

Bridge redundancy, as normally defined, is the capability of a bridge to continue to carry loads after the damage or the failure of one of its members. The capability of a bridge to continue to carry loads after a member's failure is due to its ability to redistribute the applied loads. This normally involves a potential for transverse and longitudinal redistribution. The transverse redistribution is usually a function of the longitudinal member properties, the deck slab, the effects of secondary members, and the geometric configuration of the bridge including the number of girders, girder spacing, number of spans, and the span lengths. On the other hand, the longitudinal redistribution is usually affected by the available ductility of bridge members especially at the interior supports in continuous bridges.

The need for redundancy in highway bridges can be seen from a survey by the ASCE-AASHTO Committee on Redundancy of Flexural Systems (1985) conducted on damaged bridges, which indicated that few bridge structures have collapsed when redundancy was present. The need for redundancy ability has already been recognized by AASHTO specifications (1989). AASHTO specifications (1996) for the design of highway bridges also recognized the importance of redundancy and require its consideration when designing steel bridge members. However, the specifications give little guidance on how to define redundancy and no criteria pertaining to quantifying redundancy are explicitly specified within current bridge design codes.

To the authors' knowledge, the research on the after-fracture redundancy of the two-girder steel bridges was initiated by Heins and his co-workers (1980, 1982). They concluded from elastic analysis that utilization of bottom lateral (wind) bracing system can contribute to the integrity of two-girder bridges when one of the main girders was damaged. Daniels *et al*. (1989) conducted a nonlinear analysis to evaluate redundancy of two-girder steel bridge with a near full-depth fracture in a main girder and emphasized that the bottom lateral bracing system exhibits considerable redundancy although it is not designed to carry the primary loads.

Ghosn and Moses (1998) together with Khedekar (1998) presented a method that accounts for redundancy of intact bridges under the effect of heavy loads as well as evaluating potential hazards to damaged bridges. They proposed a unique quantitative criterion for redundancy in highway bridges, which was derived from probabilistic methods in girder-type bridges. In the study, bridge redundancy was defined as a function of the probability of bridge collapse compared to the probability of first member failure. Frangopol and his co-workers (1991, 2000) also studied different redundancy measures including probabilistic as well as deterministic measures. They emphasized the importance of system redundancy rather than component safety checks in bridge design, but no guidelines were given as to an acceptable level of redundancy.

Limited experimental work has been done for the after-fracture redundancy of two-girder steel bridge. Idriss *et al*. (1995) performed a field test on the three span continuous two-girder steel bridge to be razed and tried to evaluate the effects of bridge members on the load redistribution in damaged superstructure. They concluded from the measured data that the floor beams, lateral bracing, and concrete deck transfer the loads to the intact girder, but the main load path is the fractured girder itself as it redistributes the loads longitudinally to the interior supports through cantilever action. Tachibana *et al*. (2000) conducted a laboratory test with 1/2-scale simple span two-girder steel bridge model to evaluate the load redistribution by the prestressed concrete composite deck when one of two girders was seriously damaged. In the experiment, it is notable that the bridge model does not have the bottom lateral bracing.

Actually, there is a difference of practice in two-girder bridges, that is, the lateral bracing system has been normally present in United States but it has been often omitted in many other countries.

The omission of lateral bracing seems to come from the economic point of view and the experiences that it is to a degree harmful as the fatigue cracks initiated at the junction of lateral bracing and main girders.

From the literature survey, any comparative experiments on the reserve strength of the two-girder steel bridges have not been found under the condition of with and without the lateral bracing. Especially, the simple span two-girder bridge seems to be very dangerous when damaged because it is not expected to have longitudinal redistribution ability unlike continuous span bridge.

The aim of this study is to evaluate the effect of bottom lateral bracing on the redundancy in a simple span composite two-girder steel bridge when one of the main girder is damaged due to a fatigue crack. Therefore, the bottom lateral bracing was selected as an experimental parameter and two 1/5-scale bridge specimens with and without lateral bracing have been prepared. Tests were first performed on the intact specimens without cracked girder within elastic range to investigate the effects of the lateral bracing on the load redistribution under eccentric loading. Thereafter, ultimate loading tests were conducted on the damaged specimens with an induced crack at the center of a girder. Based on the test results, the redundancy of the simple span two-girder bridges was evaluated and some conclusions are presented.

2. Structural experiments

2.1 Test specimens

For the experimental investigation of the redundancy in simple span two-girder bridge, the scale model was prepared from a prototype bridge. The prototype bridge, 50 m long and 12 m wide for two lane highway bridge, was designed by WSD to meet Korean highway bridge design code (2005). The section of the prototype bridge is shown in Fig. 1. The girder height and the girder spacing is 2.7 m and 6 m, respectively. And the nominal thickness of concrete deck (actually prestressed concrete deck) is 34 cm.

The configuration of 1/5-scale bridge specimen, 10 m long and 1.2 m girder spacing, is shown in Fig. 2. The dimension of concrete deck, 10.5 cm thick and 1.8 m wide as shown in Fig. 2(a), was

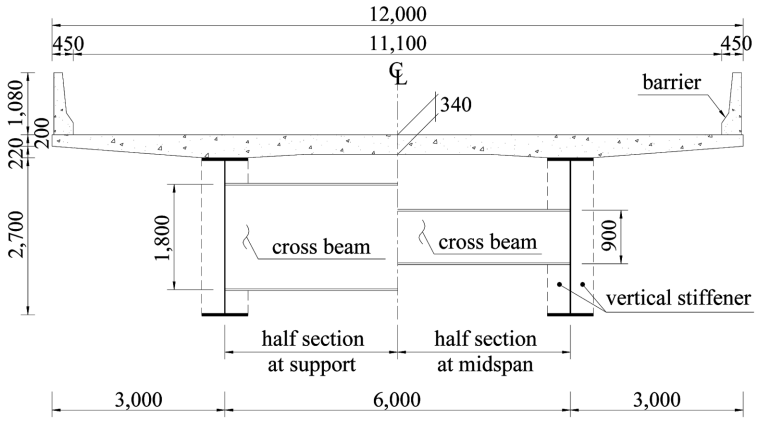

Fig. 1 Cross section of the prototype bridge (unit : mm)

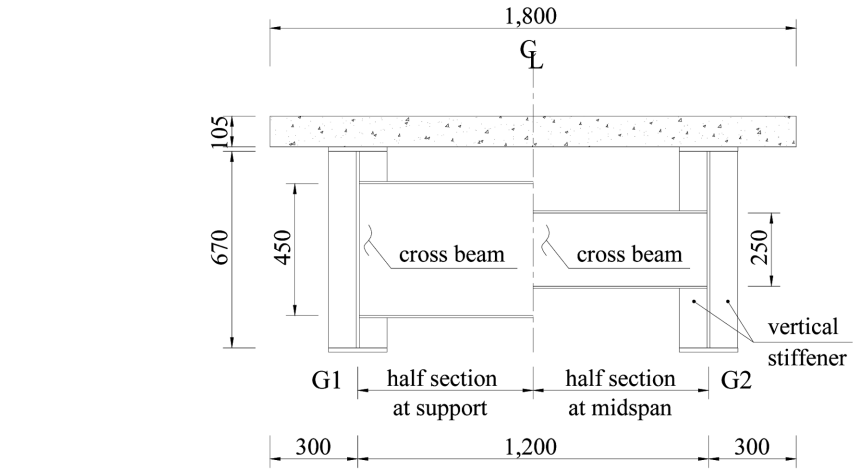

(a) Cross section

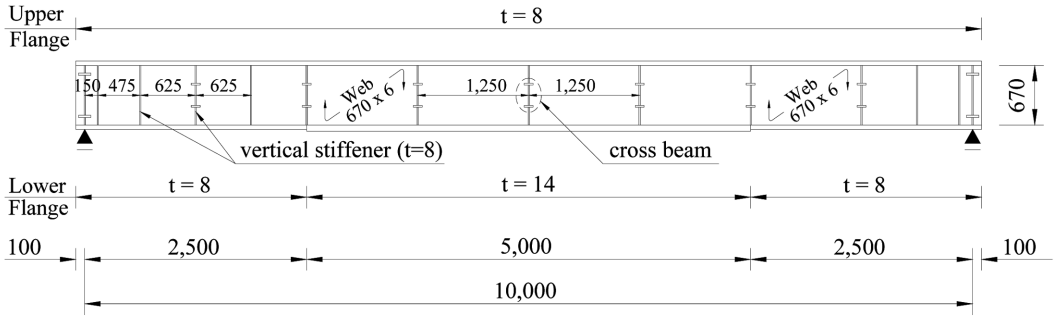

(b) Longitudinal profile of main girder

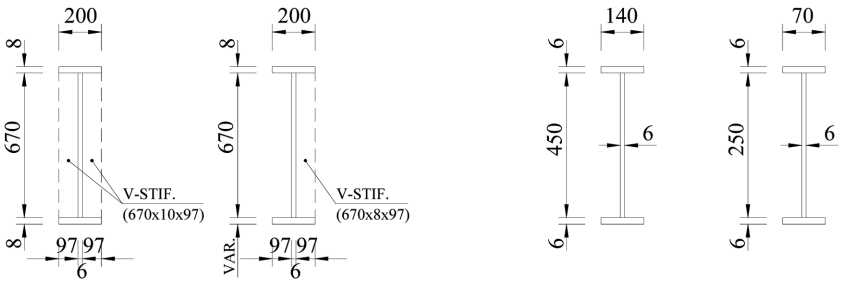

(at support) (at midspan) (at support) (at midspan)

(c) Cross section of main girder (d) Cross section of cross beam

Fig. 2 Configuration of test specimen (unit: mm)

determined to produce the same ratio of the second moment of inertia of the prototype bridge before and after composite.

The design strength of concrete was selected as 35 MPa to replicate prestressed concrete deck, but the transverse prestressing was not provided in the test specimens for simplicity. The deformed

Table 1 Strength of materials

Material \ Strength		Yield strength (MPa)	Ultimate strength (MPa)
Steel plate [1)]	6 mm	462.6	548.3
	8 mm	398.4	567.0
	14 mm	312.3	457.9
Reinforcing bar (D10 mm)		460.4	642.0
Concrete (28 days)		-	34.4

Note) 1. Design yield strength of the steel plate is 320 MPa.

reinforcing bars of 10 mm nominal diameters were installed at the top and bottom of concrete deck with a spacing of 80 mm in transverse and longitudinal direction, respectively. The reinforcement ratio amounts to 0.017 in each direction.

The thickness of girder flange and web depicted in Fig. 2(b) was determined by considering the width-to-thickness ratio in the prototype bridge. The dimension of main girder is also shown in Fig. 2(c). The vertical stiffeners were provided as shown in Fig. 2(b) and (c), which were determined from the design practice to stiffen web buckling strength.

The I-shape cross beams are installed at each 1.25 m interval to account for a typical spacing, around 6 m, in the prototype bridge. The dimensions of the end and intermediate cross beams are shown in Fig. 2(d).

For the specimen with lateral bracing, L-50 mm × 50 mm × 6 mm angles were used for brace members. The X-type bracing was adopted and the slenderness ratio amounts to about 90.

The specimens were fabricated as unshored composite girders and the shear connectors were appropriately provided not to permit slip between the concrete deck and steel girders.

Material tests were performed to evaluate the strength of steel plate, deformed bar and concrete used in the test specimens. The average strength of the materials from UTM tests for each three specimens is given in Table 1.

2.2 Test setup and test procedure

The instrumentations for measurement are shown in Fig. 3. Three displacement transducers (LVDT) were installed vertically at the lower flange of each girder and two transducers horizontally at the top and bottom flanges of each girder at the center of span to measure vertical and horizontal displacements as shown in Fig. 3(a).

The locations of strain gauges are shown in Fig. 3(b) through Fig. 3(f). In the main girders, the strain gauges were installed at the flanges and web as shown in Fig. 3(b) and 3(c). In the cross beams, the strain gauges were installed at the top and bottom flanges of cross beams at the connection with the main girders as shown in Fig. 3(d). In the bottom lateral bracing, one strain gauge per each member was installed as shown in Fig. 3(e). To measure the principal strains at the top surface of concrete deck, the strain gauges were installed in three directions at nine points as shown in Fig. 3(f). The strain gauges were also installed at the top and bottom reinforcing bars of transverse and longitudinal direction at those points.

The test specimen was supported by roller supports at both ends to simulate simple span bridge. Fig. 4 shows the bridge specimen installed for tests. Vertical load was applied by structural UTM

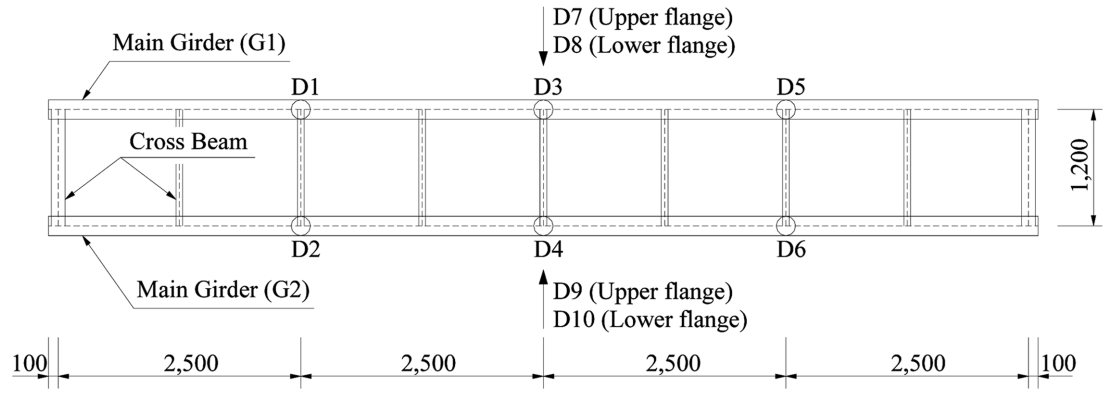

(a) Locations of L.V.D.T.

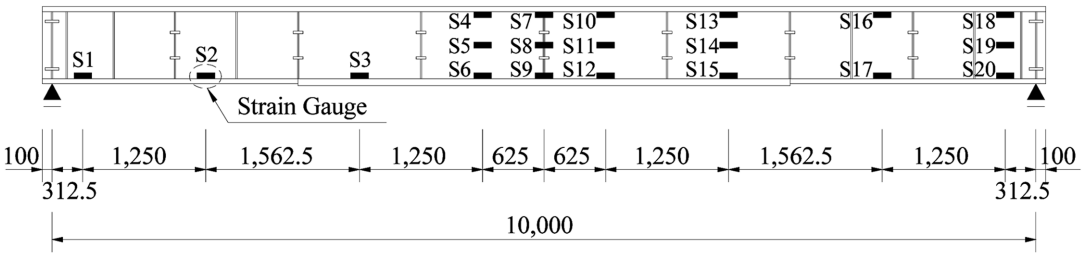

(b) Strain gauges at uncracked girder (G1)

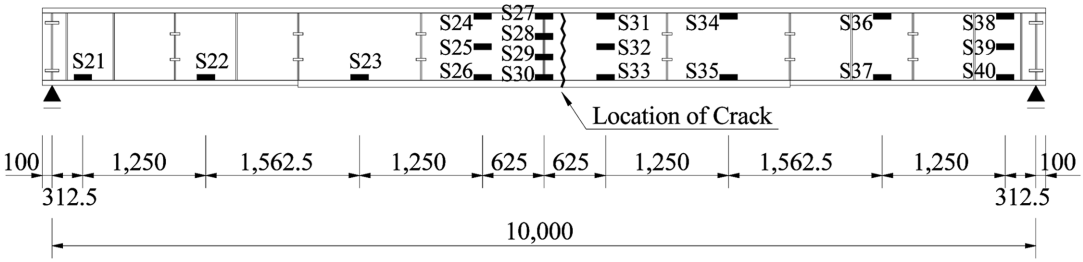

(c) Strain gauges at cracked girder (G2)

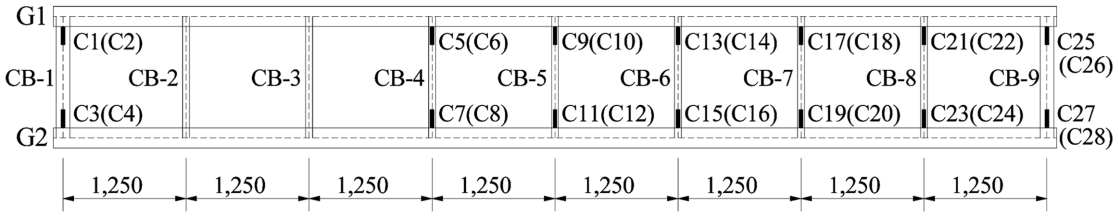

(d) Strain gauges at cross beams(Gauge No. in parenthesis corresponds to lower flange)

Fig. 3 Instrumentations (unit: mm)

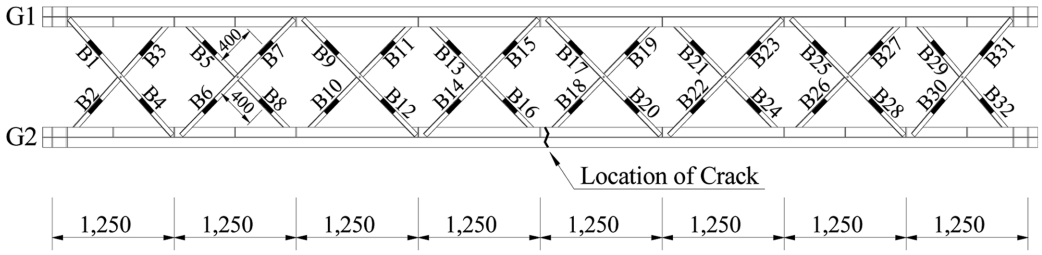

(e) Strain gauges at bracing members

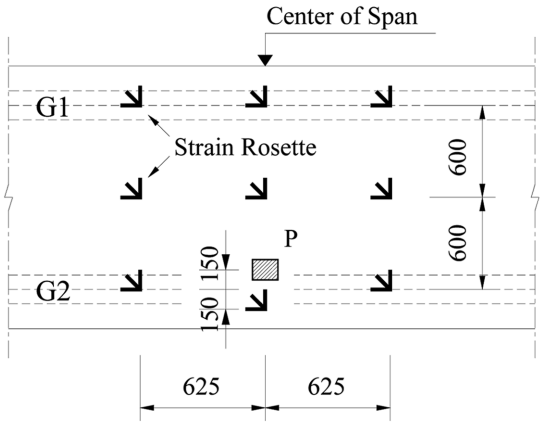

(f) Strain gauges at concrete deck

Fig. 3 Continued

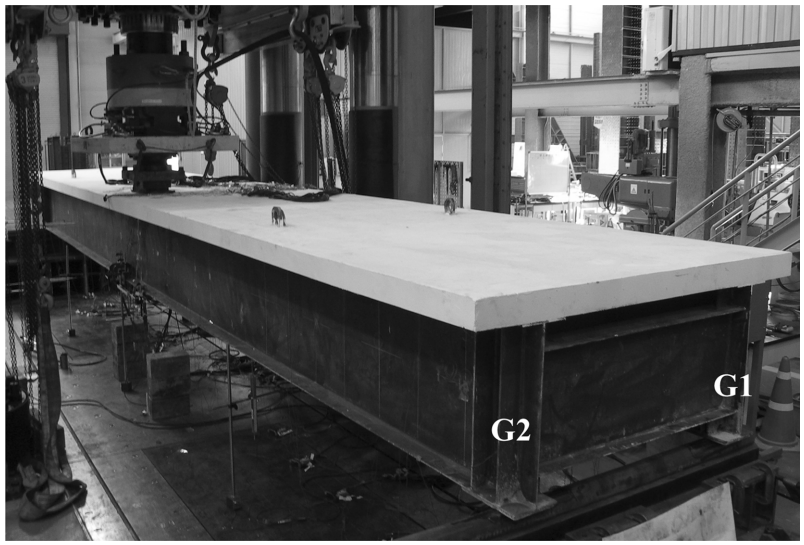

Fig. 4 Testing scene

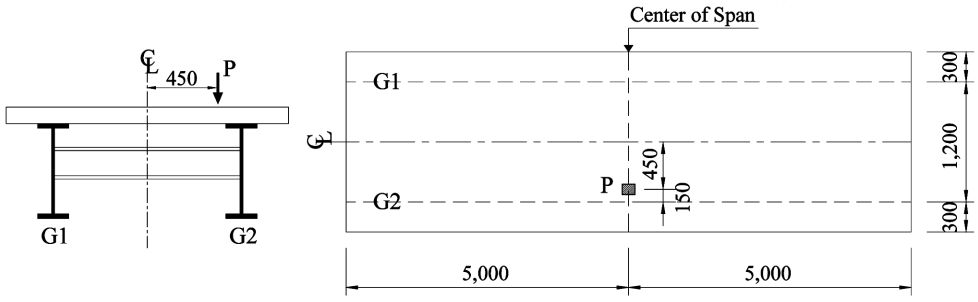

Fig. 5 Loading point (unit: mm)

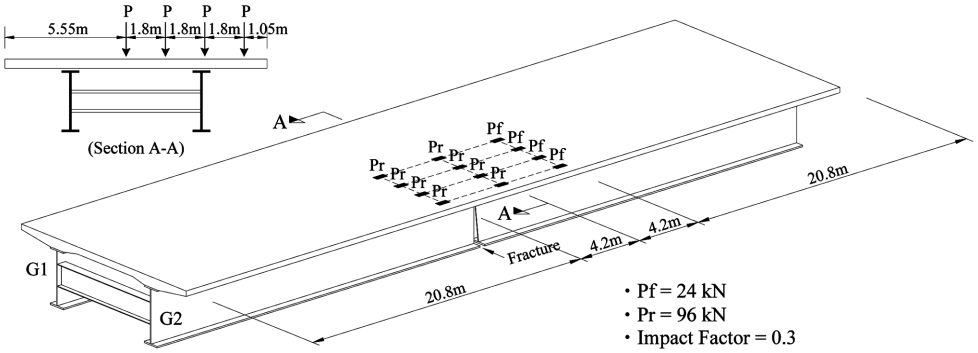

Fig. 6 Position of two side-by-side trucks for the prototype bridge

and 200 mm × 200 m × 30 mm rubber bearing was positioned between UTM head and deck surface. The loading point is the center of span in longitudinal direction and 45 cm apart from the center of deck toward the G2 girder in transverse direction as shown in Fig. 5. This loading point was determined by considering transverse eccentricity of the two side-by-side truck vehicles in the prototype bridge as shown in Fig. 6. Then, the loading ratio at the girders G1 : G2 is 1 : 7 if the RC deck is considered as simply supported by the main girders.

To investigate the effect of lateral bracing on the load redistribution during the intact condition, 200 kN force was applied with a rate of 2.5 mm/min. The loading level was determined from the preliminary numerical analysis as the bridge specimens are to be within elastic range when intact.

Thereafter, to measure the reserve strength when damaged, a near full-depth crack was introduced by torch cut in the web and lower flange of the G2 girder to simulate a severe fatigue crack. Recently, some notable researches are found to estimate the fatigue crack evolution in steel bridge by fatigue reliability analysis (Park *et al.* 2005). In this study, however, a hypothetical near full-depth crack was assumed by considering fatigue-sensitive details, and the location of crack was selected at the junction where the girder web and cross beam meet as shown in Fig. 7.

Prior to introducing the crack, temporary supports were supplied around the center of girders. The strain gauges and displacement transducers zeroing measurements were to be taken with the removal of temporary supports and readings had been then taken with loading. For the estimation of ultimate strength when damaged, the vertical load was applied with the rate of 2.0 mm/min. until the system was unable to sustain additional load any longer.

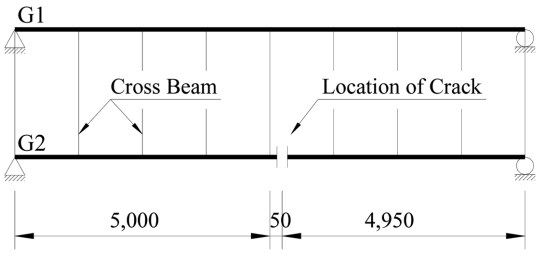

(a) Plan view

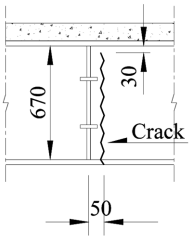

(b) Side view

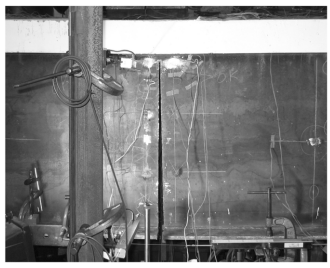

(c) Induced crack by torch cut

Fig. 7 Crack location and detail (unit: mm)

3. Test results and discussions

3.1 Load-displacements

The applied load and vertical deflections of the main girders at the center of span when intact are depicted in Fig. 8(a). The vertical deflection is 3.5 mm at the G1 girder and 11.9 mm at G2 when the lateral bracing is omitted, then the ratio of deflection is 1: 3.4. On the other hand, the deflection

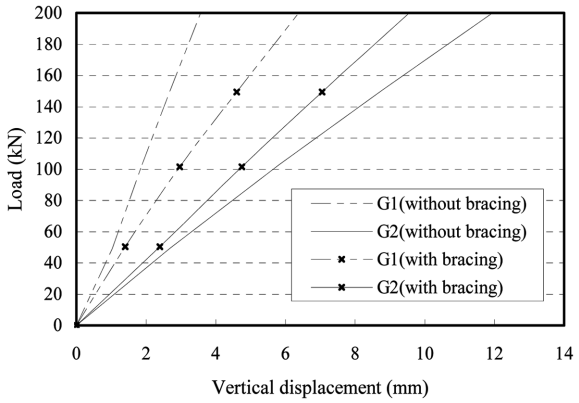

(a) Load-displacement curve(Intact condition)

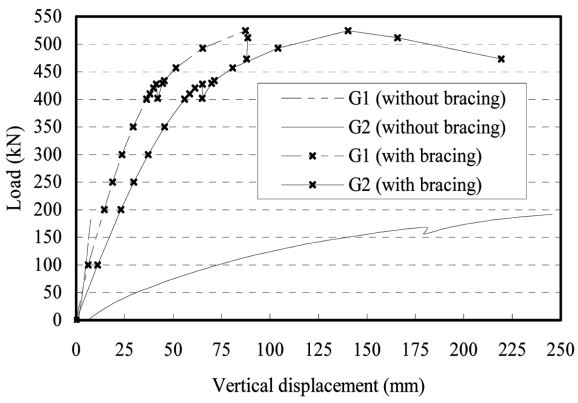

(b) Load-displacement curve(Damaged condition)

Fig. 8 Load-displacement curves

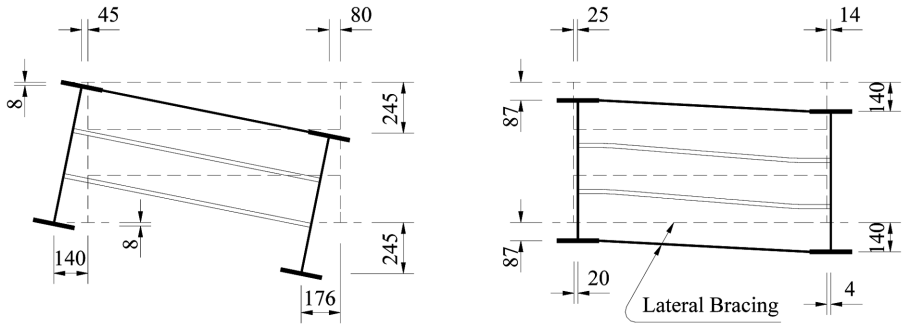

(a) without bracing (b) with bracing

Fig. 9 Deformed shape at the center of span : Damaged condition (unit: mm)

is 6.5 mm at G1 and 9.7 mm at G2 when the lateral bracing is provided, then the ratio of deflection is 1:1.5. Therefore, the deflection of G1 girder with lateral bracing is 1.8 times while that of G2 girder is 1/1.2 of that without lateral bracing. This means that the lateral bracing system redistributed the heavier loading at G2 girder to the G1 girder in intact condition.

The load-displacement curves obtained in damaged condition are shown in Fig. 8(b). From the figure, the vertical displacements under the load of 150 kN is 4.2 mm at the G1 girder and 146.7 mm at G2 in the specimen without lateral bracing, then the deflection ratio is 1:35. On the other hand, the deflection is 9.7 mm at G1 and 16.6 mm at G2 in the specimen with bracing, then the ratio is only 1: 1.7. Therefore, the deflection of G1 girder with lateral bracing is 2.33 times while that of G2 girder is only 1/8.8 of that without lateral bracing. This means that the lateral bracing played an important role to redistribute the applied load transversely in damaged condition.

Also, the ultimate load capacity of the damaged condition with lateral bracing is 520 kN while it amounts to 190 kN in the specimen without lateral bracing. Thus, the reserve strength of damaged specimen with bracing is about 2.7 times greater than that without bracing.

The deformed shapes that are traced from the measured vertical and horizontal displacements under the ultimate loads at the center of span are depicted in Fig. 9. It can be seen that the bridge model without lateral bracing behaved like rigid body while the model with lateral bracing behaved like a pseudo-closed box section. This explains that the lateral bracing stiffened the torsional rigidity of the bridge system and improved the load redistribution capability.

During the tests, undesirable punching-type failures of concrete deck around the loaded area occurred when the load reached 430 kN and 160 kN in each specimen with and without lateral bracing. These might reduce the flexural rigidity of composite girder due to partial loss of concrete deck, and some inconsistent behaviors of the structural elements after punching of deck were measured. Therefore, some of data will be presented at the load level before the punching failure for the damaged condition.

3.2 Strains of main girders

The strain distributions of girders' lower flange along longitudinal direction under 200 kN load when intact are shown in Fig. 10. In the figure, it is acknowledged that the G1 girder's strains in the specimen with lateral bracing are greater and the G2 girder's strains are less than those without

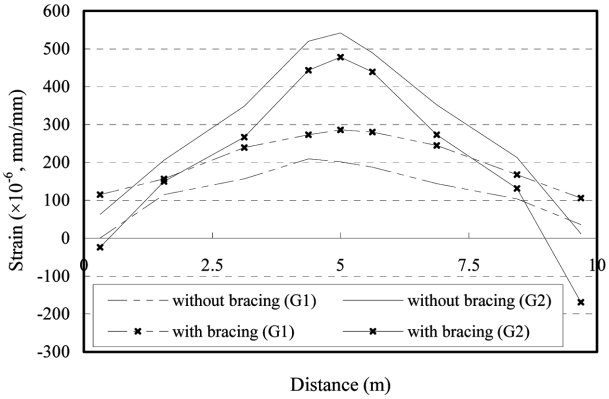

Fig. 10 Strain distributions of the girders' lower flange (intact condition, P = 200 kN)

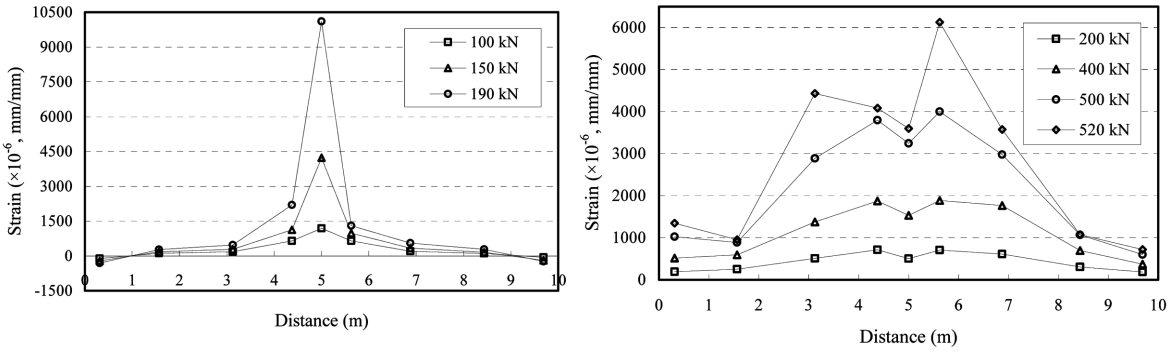

(a) without bracing (b) with bracing

Fig. 11 Strain distributions of the uncracked girder's lower flange (damaged condition)

Table 2 Strains at the uncracked girder in microstrains (Damaged condition)

Upper flange	Gauge No.	S7	S10	S13	S16
	without bracing	−268	65	54	311
	with bracing	−919	−881	−313	−237
Web	Gauge No.	S8	S11	S14	
	without bracing	695	383	315	-
	with bracing	2,343	2,766	938	
Lower flange	Gauge No.	S9	S12	S15	S17
	without bracing	10,103	1,303	560	284
	with bracing	3,567	6,223	3,610	1,021

lateral bracing. This is consistent with the girder deflections due to the improved load redistribution ability when the lateral bracing was provided.

In the damaged condition, the strain distributions of the lower flange along longitudinal direction of the uncracked girder (G1) are shown in Fig. 11, where the strains under the ultimate loads are shown, respectively. Also, the strains at the uncracked girder are listed in Table 2. From the figure and table, it is recognized that large strains (yield strain is about 1,500 microstrains for f_y =

312.3 MPa in 14 mm thick plate) were produced in the wide range of the uncracked girder (G1) when the lateral bracing was provided, while those were in narrow range, that is, just around the lower flange of the girder at span center when the lateral bracing was omitted. This means that the impact of lateral bracing on the load redistribution is significant in longitudinal direction as well as transverse direction.

The strains at the cracked girder (G2) were relatively small, i.e., less than 200 microstrains in both cases. This implies that the applied loads are mainly sustained by the uncracked girder while the cracked girder little sustain the loads in simple span two-girder bridges even when the lateral bracing was provided.

3.3 Strains of cross beams

The strains measured at the top and bottom flanges of cross beams at the connection with the main girders are listed in Table 3. In the table, the bending moments which are calculated from the measured strains are also presented in the parenthesis.

In the intact condition, it is recognized from the table that the intermediate cross beams generally acted as a cantilever beam at the connection with the G1 girder as indicated by the strain measurements at that locations in both specimens. It is also notable that the strains (also corresponding bending moments) in the specimen with lateral bracing are greater than those without lateral bracing for the same load level 150 kN. This can be explained by the deformed shape shown in Fig. 9, that is, the cross beams in the specimen with lateral bracing (box-type behavior) would sustain more loads by flexure rather than those without bracing (rigid body-like behavior).

When the crack was introduced at G2 girder, the strains (also bending moments) of cross beams increased considerably compared with the intact condition for the same load level 150 kN in both

Table 3 Strains of cross beams in microstrains

Case (Loading)	Location & Gauge No.	CB-1		CB-4		CB-5		CB-6		CB-9	
		C1	C3	C5	C7	C9	C11	C13	C15	C25	C27
		C2	C4	C6	C8	C10	C12	C14	C16	C26	C28
Intact	without bracing	−4	13	30	5	105	96	28	7	−1	−7
	(150 kN)	16	20	−7	22	−17	48	−4	16	−32	28
	Moments*	(1.2)	(0.4)	(−0.6)	(0.3)	(−2.1)	(−0.8)	(−0.5)	(0.2)	(−1.9)	(2.1)
	with bracing	−42	26	86	−49	173	31	92	−41	−56	57
	(150 kN)	28	−16	−72	40	−105	89	−93	45	66	2
	Moments*	(4.2)	(−2.5)	(−2.7)	(1.5)	(−4.8)	(1.0)	(−3.2)	(1.5)	(7.3)	(−3.3)
Damaged	Without bracing	35	144	−135	186	463	−211	−23	138	16	45
	(150 kN)	167	−49	111	−189	−486	184	155	−25	57	−42
	Moments*	(8.0)	(−11.6)	(4.2)	(−6.5)	(−16.4)	(6.8)	(3.1)	(−2.8)	(2.5)	(−5.2)
	with bracing	−76	56	102	−89	287	−304	252	−125	−90	91
	(150 kN)	72	−30	−75	78	−233	749	−236	112	111	−25
	Moments*	(8.9)	(−5.2)	(−3.1)	(2.9)	(−9.0)	(18.2)	(−8.4)	(4.1)	(12.1)	(−7.0)
	with bracing	−198	276	275	−434	1893	−702	1985	−279	−183	251
	(400 kN)	244	−117	−293	464	640	3671	−397	738	312	−62
	Moments*	(26.7)	(−23.7)	(−9.8)	(15.5)	(−21.7)	(75.6)	(−41.2)	(17.6)	(29.9)	(−18.9)

Note) *Moments in kN·m

specimens. This means that the cross beams contributed to redistribute the load to the intact girder (G1) according as the cracked girder (G2) little sustain the applied load after fracture of the girder.

The maximum strain of the cross beam in the specimen with lateral bracing reached 3,671 microstrains under 400 kN load which corresponds to about 80% of ultimate load capacity 520 kN. On the other hand, only 486 microstrains were produced under 150 kN load which is also about 80% of ultimate load capacity 190 kN when the bracing was not provided. This means that the load redistribution ability of the cross beams enhanced when the lateral bracing was provided, but the role of cross beams is relatively insignificant due to rigid body-like behavior when the bracing was omitted.

3.4 Strains of lateral bracings

The strain readings at the lateral bracing members under 200 kN load are shown in Fig. 12(a) when intact. In the figure, the tensile members are drawn by solid lines and the compressive members by dashed lines. Such results can be understood by considering that the heavily loaded G2 girder will exhibit more elongation than the G1 girder.

After the crack was introduced at the G2 girder, the strains under 200 kN load are shown in Fig. 12(b). The two diagonals in the panels at the crack experienced a drastic increase in their

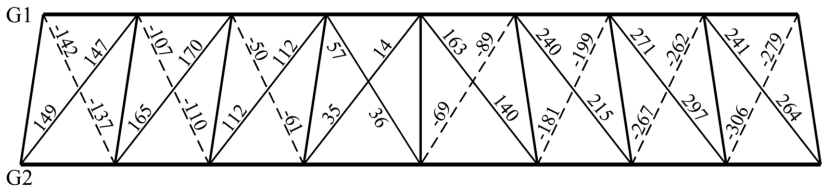

(a) Intact condition (P=200kN)

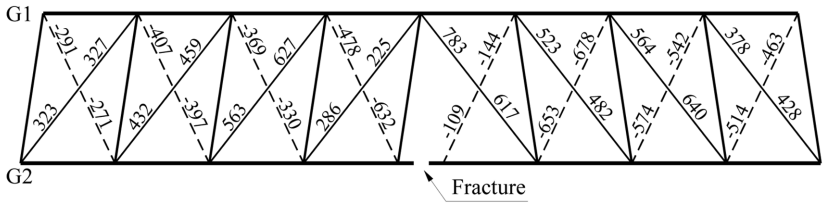

(b) Damaged condition (P = 200 kN)

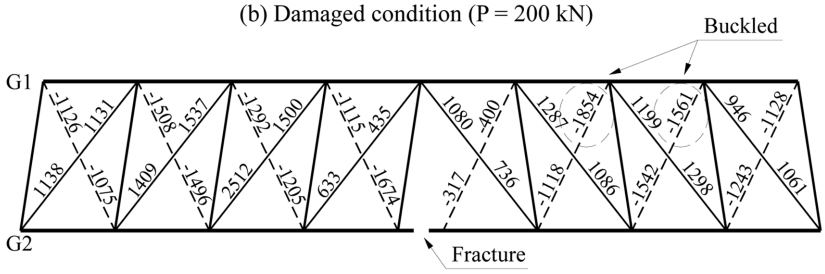

(c) Damaged condition (P=480 kN)

Fig. 12 Strains of the lateral bracing in microstrains

tensile force and the diagonals in the rest panels also show considerably increased values.

The strains of diagonals under 480 kN load, just starting the buckling of some diagonals, are shown in Fig. 12(c). From the figure, it is acknowledged that the diagonals in all panels show large strains. This illustrates that all the lateral bracing members contributed substantially to redistribute the load longitudinally as well as transversely to the intact girder G1 until the ultimate condition was reached.

3.5 Strains of concrete deck

The principal compressive strains at the top surface of the reinforced concrete deck under 150 kN load are shown in Fig. 13(a) when intact. The principal strains in the specimen with lateral bracing are larger at G1 girder location (points AL, AC, and AR) while those are smaller at G2 girder location (points CL, CC, and CR) than those without bracing. This is again consistent with the girder deflection due to the improved ability of load redistribution when the lateral bracing was present.

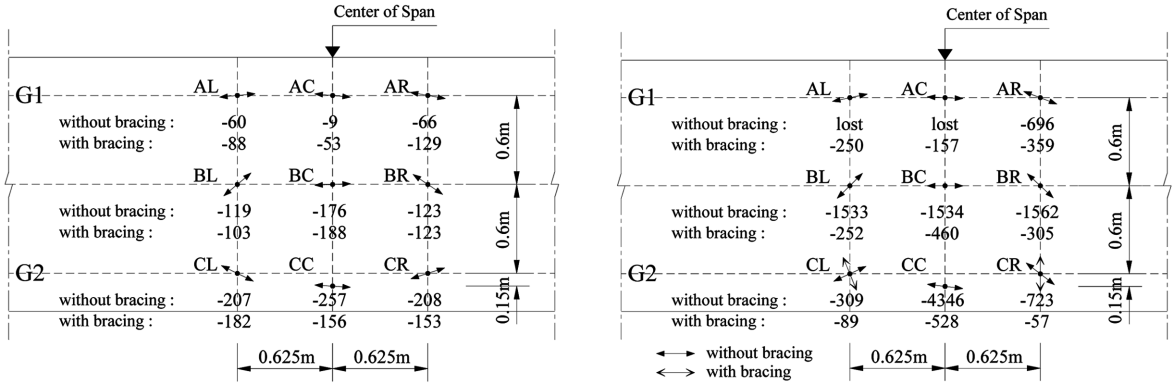

(a) Intact condition (P=150kN)

(b) Damaged condition (P = 150 kN)

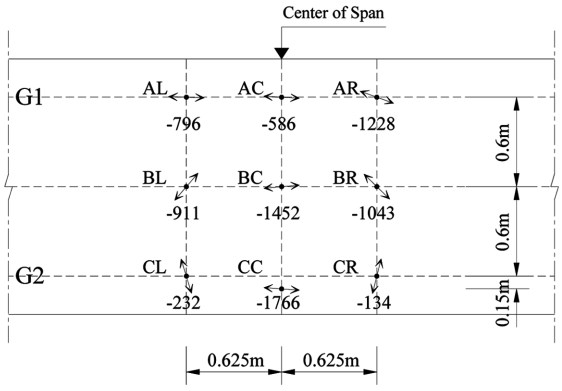

(c) Damaged condition with bracing (P = 400 kN)

Fig. 13 Principal strains at concrete deck in microstrains

Table 4 Strains of deck in microstrains (Damaged condition)

Case	Direction & Location	Longitudinal direction			Transverse direction		
		BL	BC	BR	BL	BC	BR
Without Bracing (150kN)	Concrete surface	−597	−1,534	−756	−505	−13	−179
	Upper bar	4	−143	−61	259	−29	251
	Lower bar	298	898	594	958	187	1,314
With Bracing (150kN)	Concrete surface	−95	−465	−126	−120	6	−106
	Upper bar	−110	−119	−119	−15	−25	−9
	Lower bar	−111	130	−69	171	21	218
With Bracing (400kN)	Concrete surface	−335	−1,432	−445	−453	−19	−409
	Upper bar	−312	−370	−327	10	−104	6
	Lower bar	−255	295	−110	727	588	819

The directions of the principal strains in both specimens were very similar when intact, so those are presented for the specimen without lateral bracing in the Fig. 13(a). From the figure, it is noted that longitudinal bending moments are governing at the deck area above the girders (points AL~AR and CL~CR) and at span center (points AC, BC, CC) while the other areas such as points BL and BR are supposed to undergo biaxial moments due to transverse bending moments as well as longitudinal moment.

After the crack was introduced at the G2 girder, the principal strains of the deck under 150 kN and 400 kN (for the case without lateral bracing only) loads are shown in Fig. 13(b) and 13(c), respectively. In the specimen without lateral bracing, the strain gauges in transverse direction at the points AL and AC were damaged due to tensile crack, so the strains at the corresponding points are not shown in the Fig. 13(b). From the figure, it is recognized that the deck experienced a drastic increase in their strains after fracture. It is also noted that the directions of principal strains at the points CL and CR changed especially in the model with bracing. This implies that the transverse moments occurred in the deck to redistribute the load to the uncracked girder G1 after fracture, but the magnitudes are rather smaller than other areas. Thus, it is thought that the deck and girder at these areas (points CL and CR) sustained relatively small load according as the point CC became to a hinge.

To investigate the load redistribution by the reinforced concrete deck, the strains at the points BL, BC and BR in transverse as well as longitudinal directions are listed in the Table 4. It is notable that the concrete and reinforcing bars at the points BL and BR exhibits considerable strains in the transverse direction. This illustrates that the deck away from the center of span contributed to redistribute the applied load in transverse direction as well as longitudinal direction.

Also, from the Table 4, the deck areas at the points BL and BR except the point BC are under compression throughout the full-depth of deck when the lateral bracing was provided while those are not when the lateral bracing was omitted. This implies that the bridge system with the bottom lateral bracing behaved like a composite pseudo-closed box section, thus the neutral axis located below the concrete deck.

During loading, the crushing and separation of concrete around point CC was investigated between the punching load level and the ultimate load level in both specimens.

4. Evaluation of redundancy

4.1 Redundancy criteria

As mentioned in the Introduction, Ghosn and Moses (1998) presented a unique criterion pertaining to quantifying redundancy levels, which was derived from probabilistic methods in girder-type highway bridge systems. They considered the relative safety index in Eq. (1) as a measure of redundancy, that is, the redundancy in damaged bridge can be defined as the ability of bridge system to continue to support load after the failure of its most heavily loaded member.

$$\Delta\beta_d = \beta_{damaged} - \beta_{member} \tag{1}$$

In Eq. (1), $\beta_{damaged}$ is the safety index of damaged bridge system and β_{member} is that of the member which failed first.

To determine a proper value of $\Delta\beta_d$, i.e., an adequate level of redundancy, they performed numerical analysis with the parameters; number of girders (4~10 girders), girder spacing (4~12 ft), and span length (45~150 ft). Then, they suggested a system reserve ratio R_d quantifying structural redundancy levels in damaged state of highway bridges, which was derived from Eq. (1). For details, the readers are recommended to refer to the reference (Ghosn and Moses 1998). The definition and required value of R_d for the damaged bridge not to collapse in girder-type bridges was suggested as follows.

$$R_d = \frac{LF_d}{LF_1} \geq 0.5 \tag{2}$$

where, LF_d is the live load multiplier corresponding to the ultimate capacity of the damaged bridge and LF_1 is the capacity to carry live loads before the first member failure.

The factor LF_d can be evaluated by analyzing (or experimentally) the damaged structure under the effect of dead load and live loads on a nonlinear structural model of the bridge and incrementing the live loads until the structural system collapses. The factor LF_1 can be calculated by applying the dead loads and live loads on a linear elastic model of the bridge (intact) and then incrementing the live loads until first member failure occurs. In the girder-type bridge, the main girder (heavily loaded) generally reaches first yielding and thus the LF_1 factor was defined as follows for the most heavily loaded girder.

$$LF_1 = \frac{M_R - M_D}{M_L} \tag{3}$$

where, M_R is the member's unfactored ultimate moment capacity, M_D is the member's unfactored moment by dead loads, and M_L is the member's unfactored moment by live loads.

In this study, Eq. (2) will be used to evaluate the redundancy in simple span two-girder bridge. The reason to use the equation as a measure of redundancy is that it is considered as a valid criterion derived from a probabilistic approach with the consideration of essential parameters.

4.2 Evaluation of redundancy

Based on the Eq. (2) and (3), the redundancy of the two-girder bridge will be evaluated by using

the experiment results. In the evaluation, two side-by-side truck vehicles (each weight 432 kN) as shown in Fig. 6 are assumed as rating loads for a short period under damaged condition. The impact factor is assumed as 0.3 because damaged bridges are expected to experience deflections somewhat larger than the design deflection in intact condition (Daniels *et al.* 1989). Comparing the stresses developed under the two truck loads including impact in the prototype bridge (Fig. 6) with those in the test specimen (Fig. 5), the corresponding UTM load level was determined as 52 kN for the test specimen.

The ultimate moment capacity of the composite main girder, M_R of the specimen is 1,380 kN·m where the material properties in Table 1 and concrete stress of $0.85f_c'$ for equivalent rectangular stress block are considered. Also, the dead load moment M_D is computed as 39 kN·m, and the live load moment M_L under 52 kN load is 102 kN·m. In the determination of the corresponding UTM load level and live load moment, the model without lateral bracing was used because the bracing is considered as non-primary member and Eq. (1) through Eq. (3) was derived from the models without the lateral bracing.

The results of redundancy evaluation are given in Table 5. In the Table 5, the LF_1 value seems to be somewhat large. This might come from the differences such as higher yield strength of steel plate than the design yield strength 320 MPa as shown in Table 1, application of two trucks for rating loads (three lane loading was used in design stage), and the difference of dead load, especially due to the concrete deck weight, between the prototype bridge (Fig. 1) and the test specimens (Fig. 2). Among these, calibration of the dead load is essential to estimate a proper redundancy.

Table 5 Redundancy evaluation

Case	Bracing	LF_1	LF_d	R_d
Experiment results (No dead load calibration)	w/o lateral bracing	$\frac{1{,}380-39}{102} = 13.1$	190 kN/52 kN = 3.65	0.28
	with lateral bracing		520 kN/52 kN = 10.0	0.76
Numerical results (dead load calibration)	w/o lateral bracing	$\frac{1{,}380-330}{102} = 10.3$	77 kN/52 kN =1.48	0.14
	with lateral bracing		407 kN/52 kN =7.83	0.76

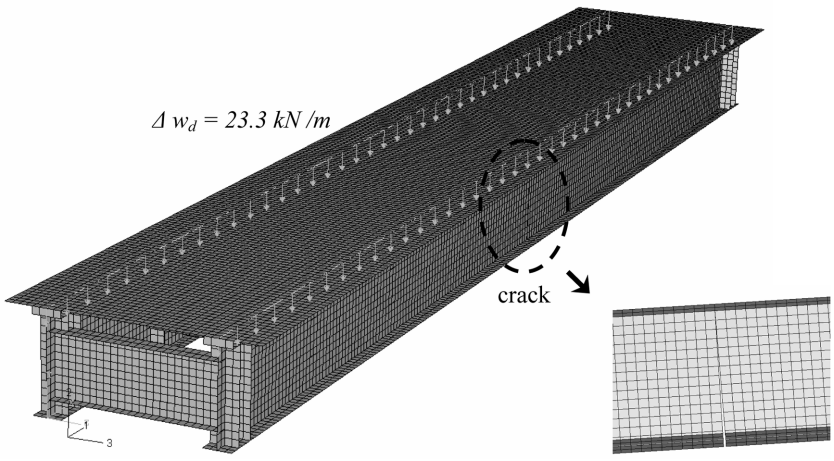

Fig. 14 Finite element model for dead load calibration

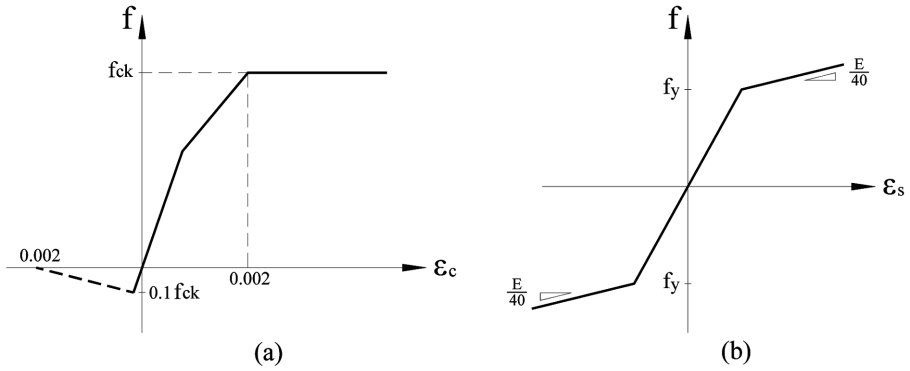

Fig. 15 Material model; (a) Concrete, (b) Steel plate and Reinforcing bar

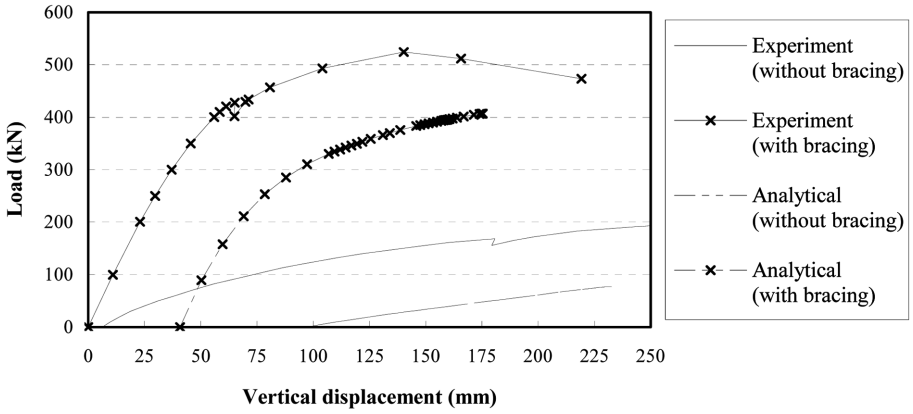

Fig. 16 Load-deflection curves at G2 girder under live loads

The corresponding stress at the lower flange of the girder under the dead load moment 39 kN·m is only 18 MPa, while it is 150 MPa in the prototype bridge. Thus, an additional dead load for the test specimen to calibrate the stress due to dead load will be considered. Finite element model in Fig. 14 (without concrete deck for unshored construction and without the crack at G2 girder for the dead load calibration) was used to determine the additional dead load by using the computer program ABAQUS (2004). It was found from the numerical analysis that the additional dead load Δw_d = 23.3 kN/m is necessary to compensate the difference of stress, 132 MPa. Then, the calibrated dead load moment becomes $\Delta M_d' = 39 + 23.3 \times 10^2/8 = 330$ kN·m.

Nonlinear analysis was performed to evaluate the ultimate load capacity with the consideration of steps; 1) loading Δw_d on the intact girders without concrete deck, 2) installation of concrete deck, 3) introduction of crack at the G2 girder as shown in Fig. 14, 4) loading at the UTM head position as shown in Fig. 5. The nonlinear analysis was also performed by the program ABAQUS and the material models for concrete and steel are shown in Fig. 15. The load-deflection curves under the load corresponding to the UTM load is depicted in Fig. 16. From the figure, the live load capacity is 77 kN for the specimen without bracing and 407 kN with bracing. Based on the numerical analysis, the redundancy was evaluated as shown in Table 5. (If the design yield strength 320 MPa for steel plate is used, M_R is 1,200 kN·m, then the LF_1 value becomes 8.5.)

When the dead load calibration is considered, the results show that the system reserve ratio R_d increases 5.4 times if the lateral bracing is provided, and the required value 0.5 is obtained. This illustrates that the lateral bracing system could secure the redundancy of simple span two-girder bridge not to collapse although it is not intended as a primary member in design practice.

5. Conclusions

An experimental approach has been conducted to evaluate the impact of the bottom lateral bracing system on the redundancy in simple span two-girder steel bridge. From the investigation of the bridge behaviors during experiments, the two-girder bridge system with the bottom lateral bracing system behaved like a pseudo-closed box girder bridge, which implies the bottom lateral bracing acts as a lower flange of box section and stiffens the torsional rigidity although it is not intended as primary member.

It was acknowledged from the experiments that the load redistribution was provided in the three-dimensional structure by the concrete deck and cross beams, and this load transfer in transverse direction occurred mainly at the vicinity of the crack. When the lateral bracing was provided, the role of the cross beams and concrete deck enhanced and it played a significant role of the load redistribution in longitudinal as well as transverse direction. The lateral bracing system was also to some degree effective for the load transfer in intact condition.

Although the load redistribution in longitudinal direction is not expected in simple span bridge unlike continuous span bridge when damaged, it was recognized that the redundancy increased by 5.4 times and an appropriate level of redundancy can be obtained when the lateral bracing is provided. Therefore, it is recommend to provide the lateral bracing in simple span two-girder bridge as a safety device not to collapse even if a serious damage occurred during the interval of inspection.

Acknowledgements

This work was supported by a grant (ø5CCTRDø9-High Performance Construction Material Research Center) from the Construction Core Technology Program funded by MOCT of Korean government.

References

ABAQUS Inc. (2004), *ABAQUS/Standard User's Manual (Ver. 6.4)*.

American Association of State Highway and Transportation Officials (1989, 1996, 2002), *Standard Specifications for Highway Bridges*.

American Association of State Highway and Transportation Officials (2004), *LRFD Bridge Design Specifications*.

Daniels, J.H., Kim, W. and Wilson, J.L. (1989), *Recommended Guidelines for Redundancy Design and Rating of Two-Girder Steel Bridges*, NCHRP Report 319, TRB.

Heins, C.P. and Hou, C.K. (1980), "Bridge redundancy: Effects of bracing", *J. Struct. Div., Proc.,* ASCE, **106**(ST6), 1364-1367.

Heins, C.P. and Kato, H. (1982), "Load redistribution of cracked girders", *J. Structu. Div., Proc.,* ASCE, **108**(ST8), 1909-1915.
Frangopol, D.M. and Nakib, R. (1991), "Redundancy in highway bridges", *Eng. J., Am. Ins. Steel Constr.*, First quarter, 45-50.
Frangopol, D.M. and Gharaibeh, E.S. (2000), "Safety assessment of bridges based on system reliability and redundancy", *Proc. of 16th Congress of IABSE*, Lucerne, September.
Ghosn, M. and Moses, F. (1998), *Redundancy in Highway Bridge Superstructures*, NCHRP Report 406, TRB.
Idriss, R.L., White, K.R., Woodward, C.B. and Jauregui, D.V. (1995), "After-fracture redundancy of two-girder bridge: Testing I-40 bridges over Rio Grande", *Proc. of the Fourth International Bridge Engineering Conference*, San Fransisco, 316-326, TRB.
Khedekar, N.C. (1998), *Redundancy for Steel Highway Bridge Superstructures*, Ph.D. thesis, Department of Civil Engineering, Case Western Reserve University, Cleveland, Ohio.
Korea Ministry of Construction and Transportation (2005), *Korean Highway Bridge Design Code*. (in Korean)
McGormley, J.C., Hill, H.J. and Koob, M.J. (2000), "The benefits of providing redundancy to non-redundant structures", *Proc. of 16th Congress of IABSE*, Lucerne, September.
Park, Y.S., Han, S.Y. and Suh, B.C. (2005), "Fatigue reliability analysis of steel bridge welding member by fracture mechanics method", *Struct. Eng. Mech.,* **19**(3), 347-359.
Tachibana, Y., Tsujikado, M., Echigo, S., Takahashi, S. and Miki, C. (2000), "A study of after-fracture redundancy for two-girder bridges", *J. Constr. Manage. Eng.,* JSCE, 241-251. (in Japanese)
Task Committee on Redundancy of Flexural Systems of the ASCE-AASHTO Committee on Flexural Members of the Committee on Metals of the structural Divisions (1985), "State-of-the-art report on redundant bridge systems", *J. Struct. Eng.,* ASCE, **111**(12), 2517-2531.